water

MDPI

Article

Francis Turbine Draft Tube Troubleshooting during Operational Conditions Using CFD Analysis

Moona Mohammadi [1,*], Ebrahim Hajidavalloo [2], Morteza Behbahani-Nejad [2], Mohammadreza Mohammadi [3,*], Saber Alidadi [1] and Alireza Mohammadi [4]

[1] Operation and Maintenance Department, Water Supply Deputy, Khuzestan Water and Power Authority (KWPA), Ahvaz 61335-137, Iran; alidadis@yahoo.com
[2] Mechanical Engineering Department, Shahid Chamran University of Ahvaz, Ahvaz 61357-83151, Iran; hajidae@scu.ac.ir (E.H.); bnmorteza@scu.ac.ir (M.B.-N.)
[3] School of Science, Engineering, and Design, Teesside University, Middlesbrough TS1 3BX, UK
[4] Generation and Transfer Planning Office, Operation Deputy, South East Company of Operation, Generation, and Transfer Water, Ahvaz 63461-15386, Iran; alireza.m6202@gmail.com
* Correspondence: moona_mohammadi@yahoo.com (M.M.); m.mohammadi@tees.ac.uk (M.M.)

Abstract: Hydropower plant vibrations due to pressure fluctuations and their troubleshooting methods are some of the most challenging issues in power plant operation and maintenance. This paper targets these fluctuations in a prototype turbine in two geometries: the initially approved design and the as-built design. Due to topographic conditions downstream, these geometries slightly differ in the draft tube height; the potential effect of such a slight geometrical change on the applicability of troubleshooting techniques is investigated. Therefore, the water flow was simulated using the CFD scheme at three operating points based on the SST k–ω turbulence model, while the injection of water/air was examined to decrease the pressure fluctuations in the draft tube, and the outputs were compared with no-injection simulations. The results show that a slight change in draft tube geometry causes the pressure fluctuations to increase 1.2 to 2.8 times after 4 s injecting at different operating points. The modification in the location of the air injection also could not reduce the increase in pressure fluctuations and caused a 3.6-fold increase in pressure fluctuations. Therefore, the results show that despite water/air injection being a common technique in the hydropower industry to reduce pressure fluctuations, it is effective only in the initially approved design geometry. At the same time, it has a reverse effect on the as-built geometry and increases the pressure fluctuations. This research highlights the importance of binding the construction phase with the design and troubleshooting stages and how slight changes in construction can affect operational issues.

Keywords: Francis turbine; vortex rope; draft tube; CFD analysis

Citation: Mohammadi, M.; Hajidavalloo, E.; Behbahani-Nejad, M.; Mohammadi, M.; Alidadi, S.; Mohammadi, A. Francis Turbine Draft Tube Troubleshooting during Operational Conditions Using CFD Analysis. *Water* **2023**, *15*, 2794. https://doi.org/10.3390/w15152794

Academic Editor: Helena M. Ramos

Received: 28 June 2023
Revised: 25 July 2023
Accepted: 27 July 2023
Published: 2 August 2023

1. Introduction

The hydropower industry plays a crucial role worldwide in the electricity market and network frequency control. Nevertheless, the technology requires complex design and construction procedures. This industry highly relies on reaction turbines (which generate combined forces of pressure and moving water), particularly Francis turbines, which offer high flexibility in a wide range of heads and discharge compared to their counterparts, e.g., Kaplan and Propeller turbines [1–3]. The initial tool that the hydropower plant designers relied on to understand the flow field through the plant elements was the Model Test. This method has been traditionally used to derive empirical equations for calculating the dimensions of hydropower turbines [4,5]. After significant development in numerical techniques and software since the 2000s, this approach has been widely used not only in the hydropower industry but also in a wide range of mechanical problems from water engineering to mechatronic and even non-Newtonian fluids due to its lower cost and faster results in comparison to experimental techniques [6–10]. Computational

tools are particularly suitable for investigating flow distribution, vortex formation, and draft tube vibration in hydropower turbines. This method has been widely used in the last two decades due to the development of powerful computational software to study fluid interaction with plant elements, including the draft tube [11–13].

The draft tube optimum geometry has been a challenging topic in the last few years, and different geometries have been examined through computational tools. At the same time, several performance criteria have been targeted in previous studies. In 2010, different elbow draft tube curvatures were selected for the Francis turbine using CFD simulation. This research found the best geometry of the draft tube based on comparing the efficiency and pressure recovery factor [14]. In another study in 2010 [15], the results of the Francis turbine for the new geometry with a narrow diffuser width and high arch door shape at the diffuser exit were compared with the traditional geometry of the draft tube using CFD simulation and validated with experimental data. The computational results show that the RANS turbulence model and steady state condition under full load agree well with the model test results. In contrast, the URANS model cannot predict suitable results for the part load. The authors suggested further investigation to obtain the best turbulence model. In 2010, the optimum ratio of the height of the draft tube to the runner diameter and the draft tube's length was computed using CFD simulation in a no-pier draft tube. The results show that the optimum height ratio is 2.24 and the optimum length ratio is 6.0, and a change in mass flow rate does not affect efficiency or loss in the draft tube. This research aimed to examine the ability of CFD simulation in complex geometry [16]. Two geometrical configurations of the elbow draft tube in the Kaplan turbine were investigated in 2012. The research's main target was to find the reasons for the drop in efficiency in the draft tube's elbow [17]. The effect of the conical draft tube and diffuser angle was investigated in the straight conical draft tube in 2012 using CFD simulation. The results show that both of the investigated parameters have significant effects on the performance of the draft tube [18]. In 2013, using CFD simulation in Francis Turbine, the vortex rope and pressure distribution of three types of guide vanes were investigated on three draft tube types: zero, one, and two piers. To develop the results, the authors suggested performing the experimental work [19]. The researcher investigated the effects of changing the draft tube diffuser on performance in 2014. The results show that the maximum efficiency was achieved in the draft tube length at 10.0 times the runner diameter. Also, the pier's location after the elbow affects the velocity distribution significantly [20]. In 2015, CFD schemes were used to find the Francis turbine draft tube's flow field behavior and performance with Splitter at different locations in the elbow. Using the horizontal Splitter in the elbow causes the outlet flow to be uniform, but the efficiency of the turbine and draft tube decreases [21]. Using CFD simulation, the design of the draft tube shape in the Francis turbine across rehabilitation was optimized in 2016. This research aimed to reduce flow loss and improve efficiency and energy recovery [22].

CFD simulation and experimental methods were used to investigate the conical draft tube, cone angle, and outlet cross-section to determine the best efficiency point in 2017. The best cone angle has been reported as 7 to 8 degrees, and it was found that increasing the cone angle degree caused decreased efficiency and backflow creation [23]. Moreover, in 2018, the Francis turbine draft tube height, length, elbow curvature radius, and outlet cross-section were targeted to optimize the draft tube design. It was found that the draft tube height of the inlet cone section, the width of the outlet section, and the elbow section curvature radius significantly affect the draft tube's performance [24]. Additionally, three types of elbow curves were studied to investigate Francis turbine efficiency in 2018. It was found that the draft tube in logarithmic spiral and hyperbolic–logarithmic spiral templates has the lowest loss coefficient and the highest efficiency, respectively [25].

Although the previous research discussed the optimization of draft tube geometries and considered various influential factors in the initial design procedure, they all ignored the slight modifications that can occur in the 'as built' designs due to construction challenges, while the potential effect of such modifications on the operation and maintenance

stages is unknown. It is a crucial piece of knowledge that links the design, construction, and operation phases, potentially influences the construction procedures, and introduces a new source of problems for troubleshooting purposes. Nevertheless, due to the interdisciplinary nature of the issue, this factor has always been overlooked.

This paper targets this significant gap and aims to investigate the potential effect of slight design modifications in the construction phase on flow characteristics; moreover, in a real industrial case based on numerical simulations, the applicability of troubleshooting methods is also investigated. Accordingly, despite the literature, this paper considers the slight differences between 'initial design' and 'as-built design' and uses CFD simulations in both geometries. The present study has mainly targeted the effect of increasing draft tube height on important flow characteristics. The current research has particularly aimed to shed light on pressure fluctuations and vortex rope, as these flow characteristics have never been investigated in the literature, and a deep understanding of these factors is essential to establishing a robust knowledge of draft tube vibrations. Additionally, the effect of air/water injection (as a common troubleshooting technique) is investigated in two geometries. Accordingly, the methodology and simulation specification are presented in Section 2. Later, the results are presented and discussed in Section 3, and the conclusions are made in Section 4.

2. Methodology

A prototype Francis turbine at the Maroon Power Plant in Khuzestan Province, Iran, was investigated in this research. Table 1 shows nominal specifications based on the design parameters of the Maroon turbine. The studies in this particular power plant show that vortex-induced vibrations are a significant problem in this plant. Therefore, investigating the issue and finding a solution would be a point of interest to both researchers and industrial applications.

Table 1. Maroon hydropower design specifications.

Power (M.W.)	Specific Speed	Speed (rpm)	Discharge (m^3/s)	Head (m)
75	172	250	70	121

The simulation was carried out in both steady and unsteady conditions. In the former, the domain included the spiral case, the stay vanes, the guide vanes, the runner, and the draft tube (Figure 1a), while in the latter, the stay vanes to the draft tube outlet were simulated (Figure 1b). Figure 1c,d show the runner and draft tube dimensions.

Governing equations, including the continuity, momentum, and turbulence equations, are required for the flow field simulation. Reynolds-averaged Navier–Stokes equations for an incompressible and Newtonian fluid are as follows [26]:

$$\frac{\partial \overline{u}_i}{\partial x_i} = 0 \tag{1}$$

$$\frac{\partial \overline{u}_j}{\partial t} + \overline{u}_i \frac{\partial \overline{u}_j}{\partial x_i} = -\frac{1}{\rho}\frac{\partial \overline{p}}{\partial x_j} + \frac{\partial}{\partial x_i}\left[\upsilon\left(\frac{\partial \overline{u}_j}{\partial x_i} + \frac{\partial \overline{u}_i}{\partial x_j}\right) - \overline{u_i' u_j'}\right] \tag{2}$$

where ρ is density, υ is kinematic viscosity, $\overline{u}$ is the average velocity, and $\overline{p}$ is the average pressure.

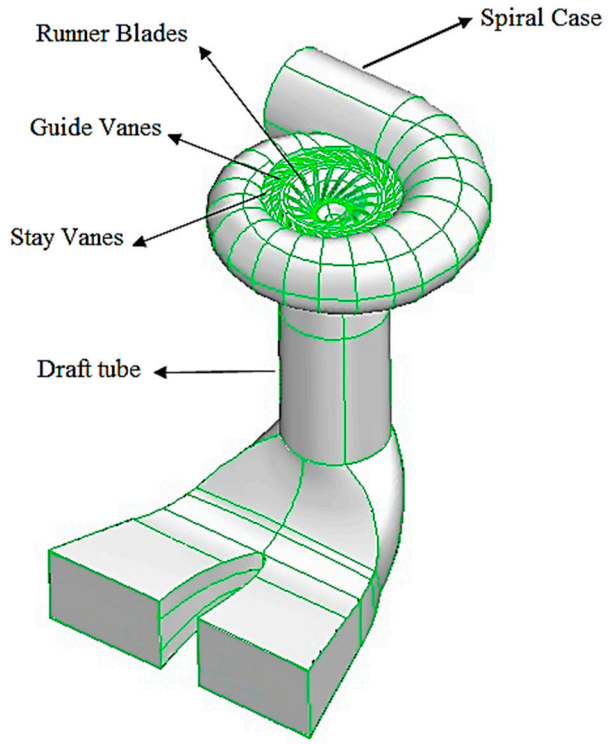

(**a**)

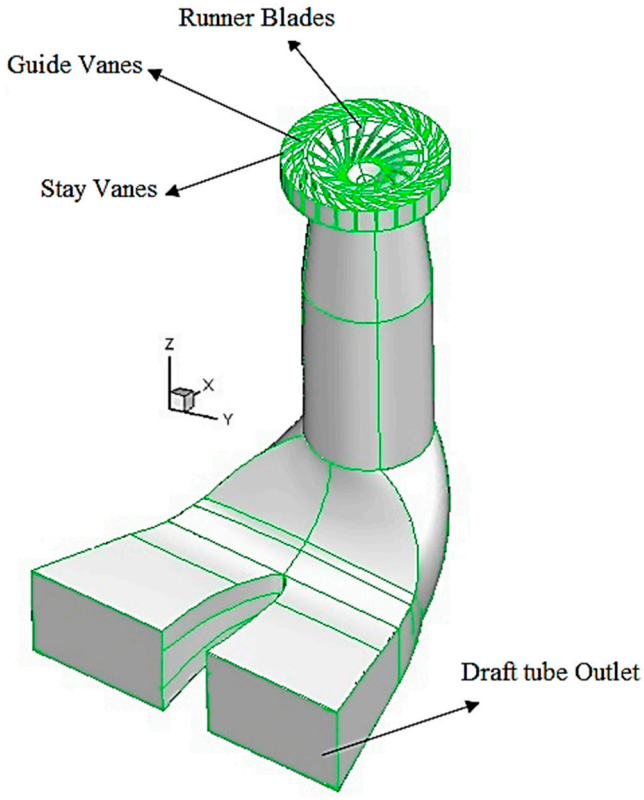

(**b**)

Figure 1. *Cont.*

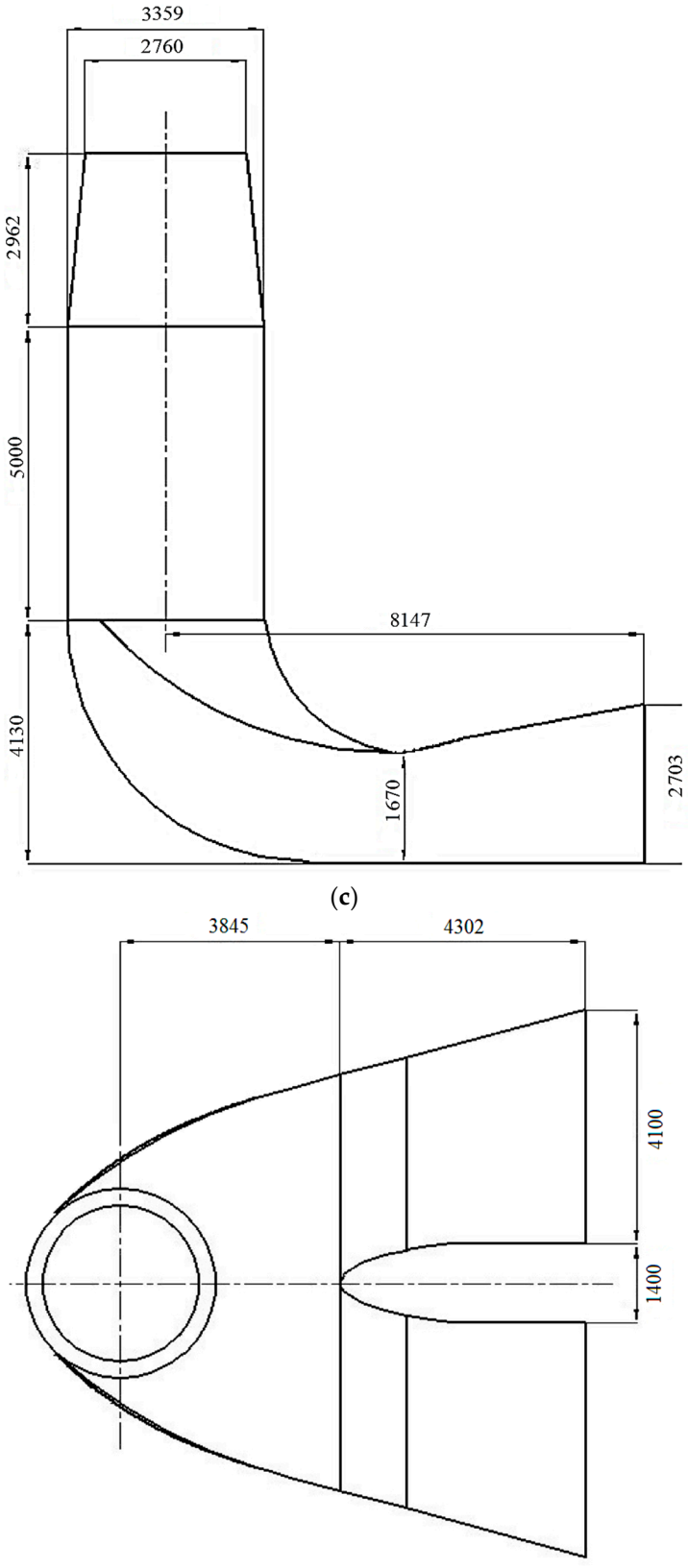

Figure 1. Maroon power plant geometry: (**a**) from the spiral case to the draft tube outlet; (**b**) from stay vanes to the draft tube outlet; (**c**) side view dimensions of the draft tube (in millimeters); (**d**) upper view dimensions of the draft tube (in millimeters).

Using the Boussinesq equation and the Reynolds stress tensor, $\overline{u_i' u_j'}$ is obtained as [26]:

$$-\overline{u_i' u_j'} = \upsilon_t \left(\frac{\partial \overline{u_i}}{\partial x_j} + \frac{\partial \overline{u_j}}{\partial x_i} \right) - \frac{2}{3} k \delta_{ij} \tag{3}$$

$$\upsilon_t = C_\mu \frac{k^2}{\varepsilon}, \; C_\mu = 0.09 \tag{4}$$

υ_t, ε, and k are kinematic turbulence viscosity, turbulence dissipation rate, and turbulence kinetic energy, respectively.

Mass flow inlet, turbulence kinetic energy (k), and specific dissipation rate (ω) were considered for spiral case inlet boundary conditions. The turbulence kinetic energy and specific dissipation rate are obtained below [27]:

$$k = \frac{3}{2} u_{ave} I^2 \tag{5}$$

$$\omega = \frac{k^{1/2}}{C_\mu^{1/4} l} \tag{6}$$

where u_{ave} is average velocity. Moreover, I and l, the turbulence intensity and turbulence length scale, respectively, are calculated below [27]:

$$I = 0.16 \left(Re_{D_h} \right)^{-1/8} \tag{7}$$

$$l = 0.07 D_h \tag{8}$$

Here, D_h is the hydraulic diameter. The outlet boundary condition was calculated based on pressure, turbulence intensity, and turbulence length scale.

The pressure value is calculated at three operating points according to Equation (9) [28], Table 2, and Figure 2.

$$\frac{p_2}{\gamma} = \frac{p_a}{\gamma} + L \tag{9}$$

where L is the distance between the tailrace and the midline of the draft tube outlet elevations, p_2 is the draft tube pressure outlet, and p_a is atmospheric pressure. The draft tube's upper and lower edge elevations are 349.5 and 346 m above sea level, respectively. In Table 2, the percent of partial discharge operating point is explained as the discharge of the turbine over optimum efficiency discharge ($Q/Q_{opt} \times 100$).

Table 2. The tailrace level at three operating points.

Operating Point (%)	Power (M.W.)	Head (m)	Tailrace (masl)
66.6	40	95	362.5
86.2	62	110.8	363.6
100	75	121	362.5

A total cell number of 2,631,341 was selected, considering grid quality and the grid independence test, using an analysis of the grid convergence index (GCI) as mentioned in detail in [29,30]. Moreover, structured and unstructured grid types were used in the draft tube and the rest of the geometry, respectively. The tangential, radial, and axial velocities, TKE (Turbulence Kinetic Energy), and ω at the beginning of the stay vanes were extracted at three operating points in the inlet of steady state.

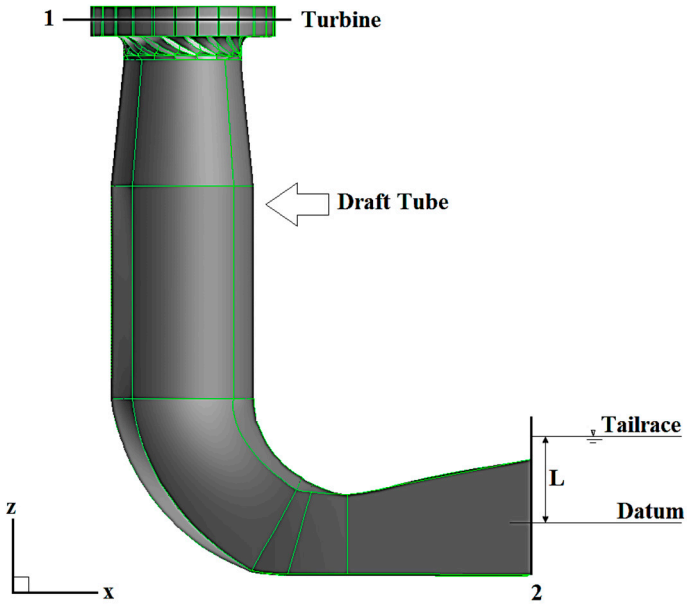

Figure 2. A 2D view of the draft tube, L, which is the distance between the mid-line of the draft tube and the tailrace.

By eliminating the spiral case, the flow was simulated from the stay vanes to the draft tube outlet in an unsteady state. Without the spiral case, the number of cells was reduced by 2,120,295, and the program run time was reduced by 41%. Therefore, the spiral case was not considered in an unsteady state simulation because of the shorter program running time.

In the current research, y+ was used 50 because this value equals the wall function schemes under no transitional flow conditions and the SST k–ω model [27,29].

Three methods can be used for validation, as mentioned in [29,30]. In the first method, which is based on the ASME standard [31], the accuracy of the current simulation was verified by comparison with EPFL University's draft tube model simulation results, as experimental data are available for the EPFL model. In the second method, the static pressure obtained from the pressure gauge installed 1 m below the turbine band was used to compare the simulation results with the experimental data [29]. In the third approach (based on the Winter–Kennedy method), the pressure difference between two points on the spiral case was compared with the simulation results [29,30]. The flow in the EPFL draft tube model was simulated in the first method using the SIMPLE algorithm and various turbulence models such as SST k–ω, RNG, k–ε, RSM, and Realizable. Different discretization schemes were implemented, such as power law, second-order upwind, MUSCL, and QUICK. Later, the results were compared with the experimental values. The comparison showed that the SST k–ω model and the power-law discretization scheme have the best outcome [29,30].

In addition to comparing the simulation results with experimental data, an analysis of the iterative convergence error value in the EPFL model is obtained with Equation (10) [30]:

$$e_i = \frac{MSR}{TMF} \tag{10}$$

MSR and TMF are the residual sources of mass and mass flux through the domain, respectively. The results show that for the SST turbulence model, the iterative convergence error for the power law is smaller (Iterative convergence error = 8.95×10^{-6}) than the value obtained for the second-order (Iterative convergence error = 1.1×10^{-4}). Consequently, the power law method demonstrates a more accurate response [29,30].

For the second method, comparisons of the simulation with experimental results at three operating points of the Maroon Power Plant (66.6%, 86.2%, and 100%) were performed,

giving resulting errors of 8%, 12.7%, and 19.3% for the three operating points, respectively (Table 3). Therefore, the results are within an acceptable range [29,30].

Table 3. Comparison of simulation and measurement values at tree operating points [29].

Operating Points (%)	Simulated Value (bar)	Measurement Value (bar)	Error (%)
66.6	1.63	1.5	8
86.2	1.7	1.5	12.7
100	1.8	1.5	19.3

In addition to the above procedures, the Winter–Kennedy method was used to estimate the accuracy of the results. In this method, the difference in pressure between two points in the hydropower plant is calculated as follows [29,30,32]:

$$Q = m\Delta p^n \quad (11)$$

Measuring the pressure difference in the Maroon hydropower spiral case gives m = 9.004523 and n = 0.5 [32]. In Equation (11), Q and Δp are the inlet turbine flow rate and the difference in pressure between the two points in the spiral case, respectively. The errors calculated at the three operating points (66.6%, 86.2%, and 100%) are 13.8%, 9.8%, and 6.23%, respectively (Table 4). Consequently, the determined errors are within an acceptable range [29,30].

Table 4. Comparison simulation and calculated values at three operating points [29].

Operating Points (%)	Calculated Value (kPa)	Simulated Value (kPa)	Error (%)
66.6	26.8	23.1	13.8
86.2	44.9	40.5	9.8
100	60.43	56.66	6.23

The time-step length is considered the time required for a one-degree runner rotation (0.00208 s) [12,29,30]. Using FLUENT 6.3.26 and two single computers with an i7-4790 CPU at 3.6 GHz, the residuals and maximum sub-iteration convergence criteria were considered 10^{-8} and 20, respectively. Each time step took about 240 s. The unsteady-state solution proceeded for up to 5 s; no significant changes were observed in the flow parameters after this time.

After the flow field simulation at three operating points, the injection water and air were added from the center of the runner cone and from 72 nozzles on the perimeter of the draft tube from the discharge ring, respectively [29]. The amount of water/air injection at three operating points is shown in Table 5. The selection of air, water, or combined air and water injection in different conditions was based on the reasons presented by [29,30].

Table 5. Percent of air and water injection at three operating points.

Operating Point (%)	Percent of Air Injection (%)	Percent of Combined Air and Water Injection (%)
66.6	-------	Air (1.5) & Water (0.6)
86.2	0.75	-------
100	0.75	-------

3. Results

The axial static pressure contour and vortex rope in the draft tube are shown in Figure 3a–c. As expected, increasing the guide vane opening degree causes a low-pressure

area and the vortex rope size to decrease. In previous research, the vortex rope in overload conditions has an onion shape [33,34]. The results of the current study (Figure 3c) align with this finding.

After flow simulation without injection, water/air injection was added based on Table 5 at three operating points. At 86.2% and 100% operating points, air injection from 72 nozzles on the perimeter of the draft tube from the discharge ring was considered, and at the 66.6% operating point, combined air and water injection were considered. Water was injected from the center of the runner cone. Figure 4a–c show pressure fluctuations on the wall at 2.3 m below the draft tube inlet and with and without injection at three operating points. The results show that pressure fluctuations increase gradually at the different operating points. Four seconds after beginning injection, pressure fluctuations increase from 1.2 to 2.8 times higher compared to the first second of injection.

The location of air injection was changed to the runner cone center to find the reason for the increasing pressure fluctuations.

The flow was simulated again without and with air injection at the 86.2% operating point. Nozzle diameter and air velocity are unknown when air is injected from the center of the runner cone. Thus, using the Strouhal number similarity, there is a similarity between two conditions: air injection from the discharge ring and the runner cone's center. Equations (12) and (13) show the relations between the Strouhal number and the discharge of the nozzle [34]:

$$St = \frac{fl}{u} \tag{12}$$

$$Q = uA \tag{13}$$

St, f, l, u, A, and Q are Strouhal numbers, rotation frequency, characteristic length (hydraulic diameter), velocity, area based on air nozzle diameter, and air discharge, respectively.

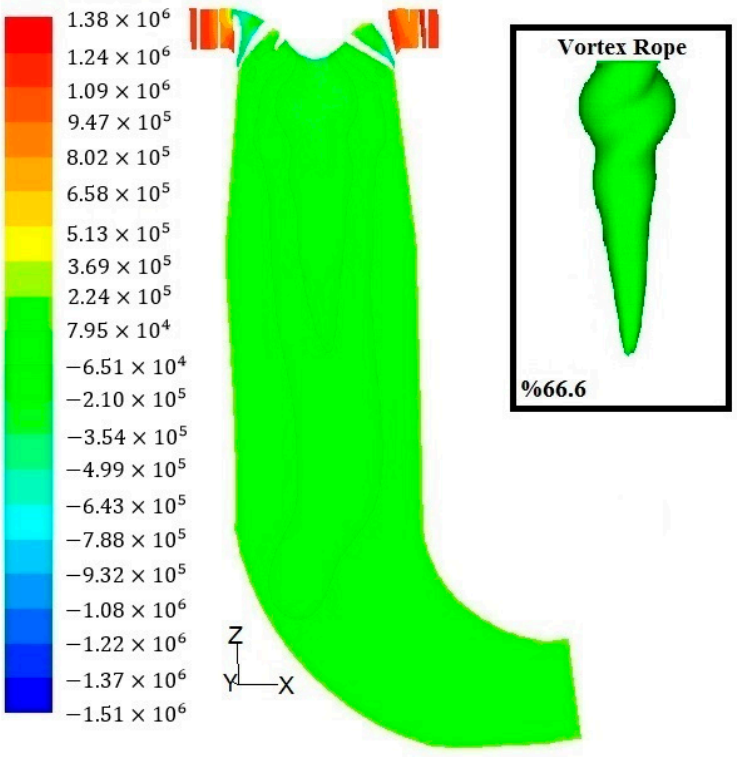

(**a**)

Figure 3. *Cont.*

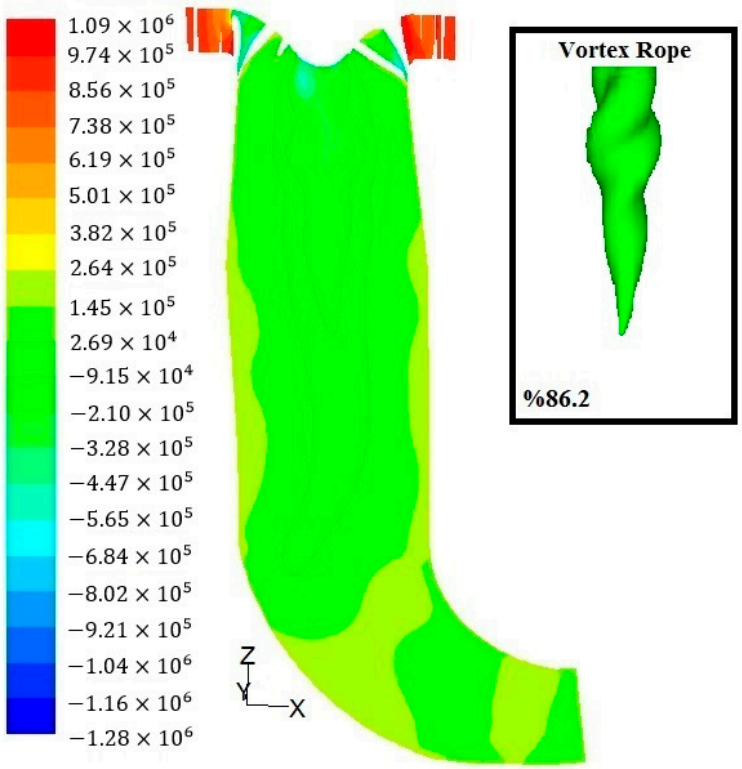

(**b**)

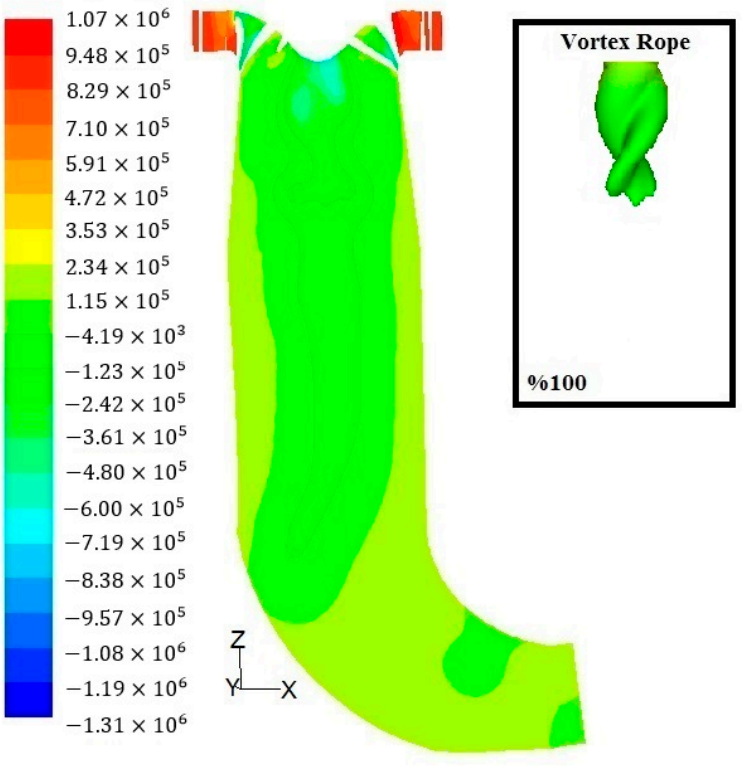

(**c**)

Figure 3. Axial static pressure contour and vortex rope: (**a**) at 66.6% operating point, (**b**) at 86.2% operating point, and (**c**) at 100% operating point.

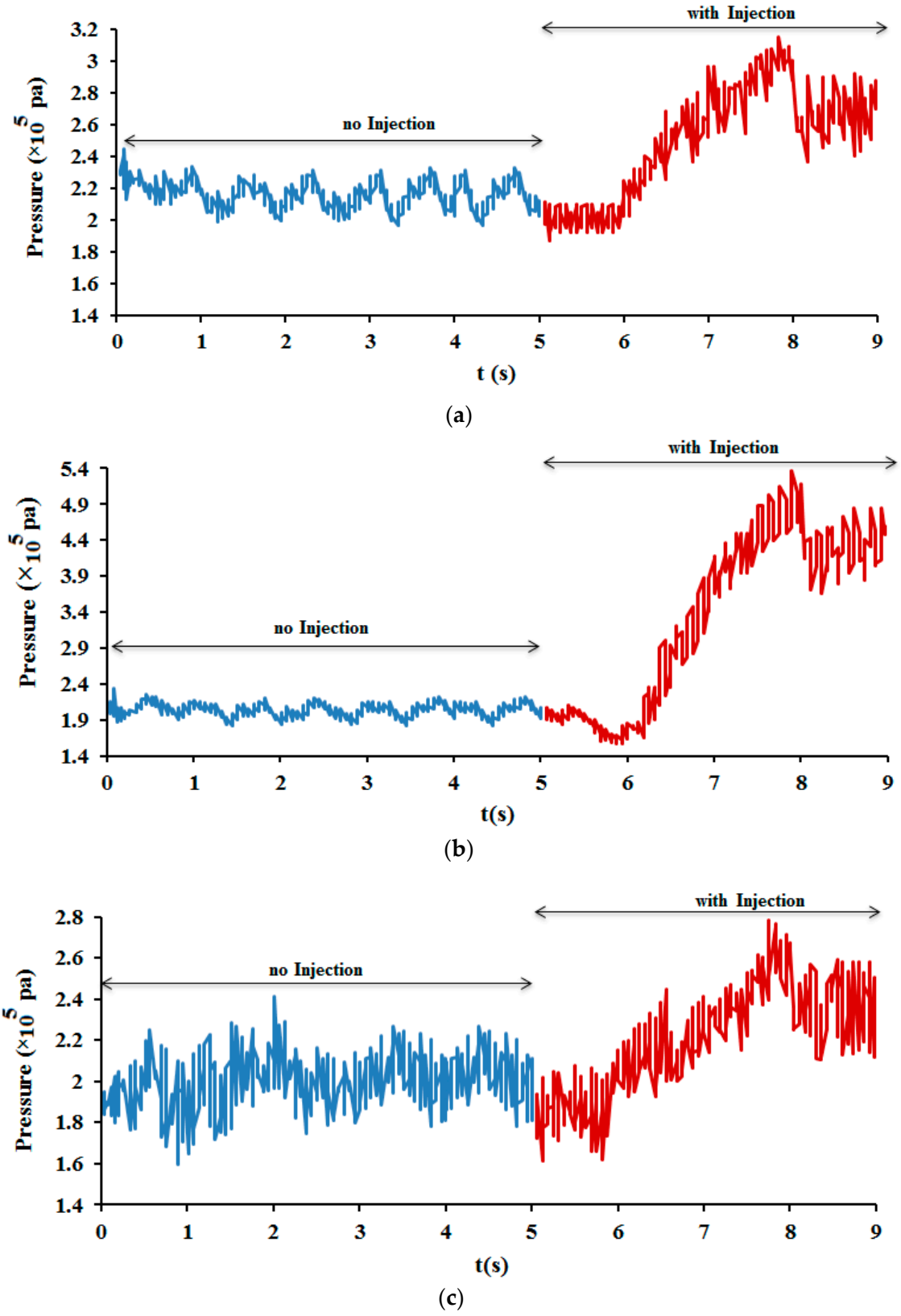

Figure 4. Pressure fluctuations on the draft tube wall at 2.3 m below the draft tube inlet, (**a**) at 66.6% operating point, (**b**) at 86.2% operating point, and (**c**) at 100% operating point.

Note that, in injection from the perimeter of the draft tube, the air was injected from 72 nozzles whose discharge and velocity have known data, whereas, in air injection from the runner cone center, both nozzle diameter and air velocity are unknown [29,30].

Pressure fluctuations on the draft tube wall during air injection from the runner cone center are shown in Figure 5. Similar to previous results, injection from the runner cone center still causes increasing pressure fluctuations.

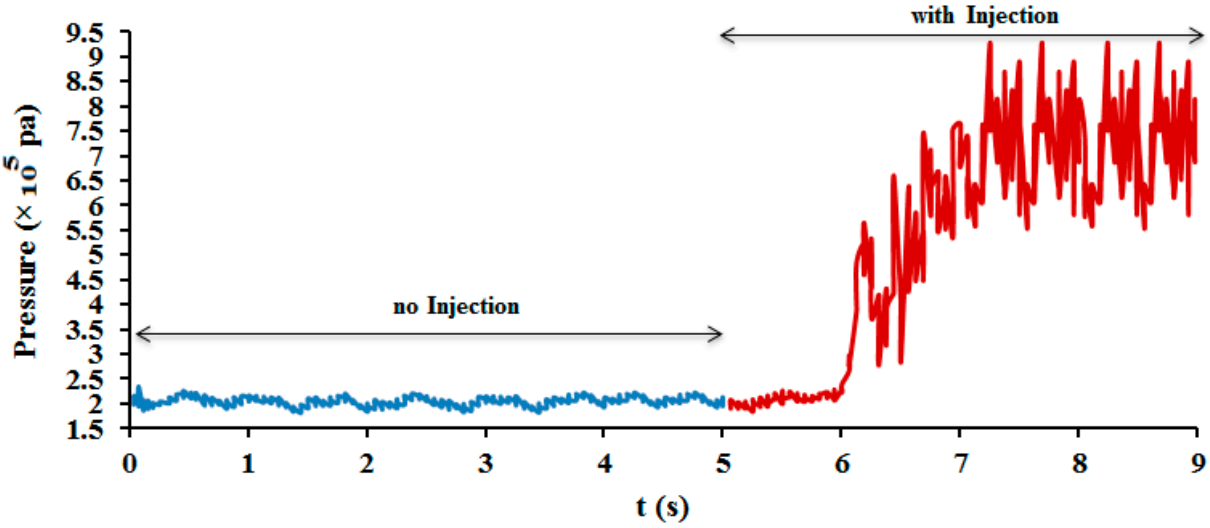

Figure 5. Pressure fluctuations on the draft tube wall at 2.3 m below the draft tube inlet, air injection from the center of the runner cone, at 86.2% operating point.

Previous research shows that injection from the runner cone center causes increasing flow turbulence in the center of the draft tube and vortex rope area [29,35]. Figure 5 demonstrates that the ratio between the second four and the second one after injection is approximately 3.6. Therefore, it is consistent with previous research.

The obtained results show that, despite injection causing decreasing pressure fluctuations on the draft tube wall, pressure fluctuations were increased in this study. Regarding the obtained results, changing the air injection location does not affect increasing pressure fluctuations. Another scenario was followed to find the reason. Accordingly, all as-built and initially approved design drawings were investigated, and it was found that there was a slight change in the height of the draft tube during execution [36]. Figure 6 shows the difference between initially designed geometry and as-built geometry. Due to the topography of the draft tube installation location and the requirement of the installation of the draft tube in unit 1 and the draft tube in development in unit 2 at the same elevation, a change in draft tube height was considered and caused 5 m differences between as-built and initially approved designs in unit 1.

The flow field was simulated again to investigate the potential effect of such a slight difference on the results by removing the extra part at the operating point of 86.2%. Figures 7 and 8 show pressure fluctuation on the draft tube wall (without and with air injection), axial static pressure contour, and vortex rope. According to Figure 7, the increasing trend is not observed after injection, and the pressure fluctuations have decreased. Also, a shorter vortex can be seen.

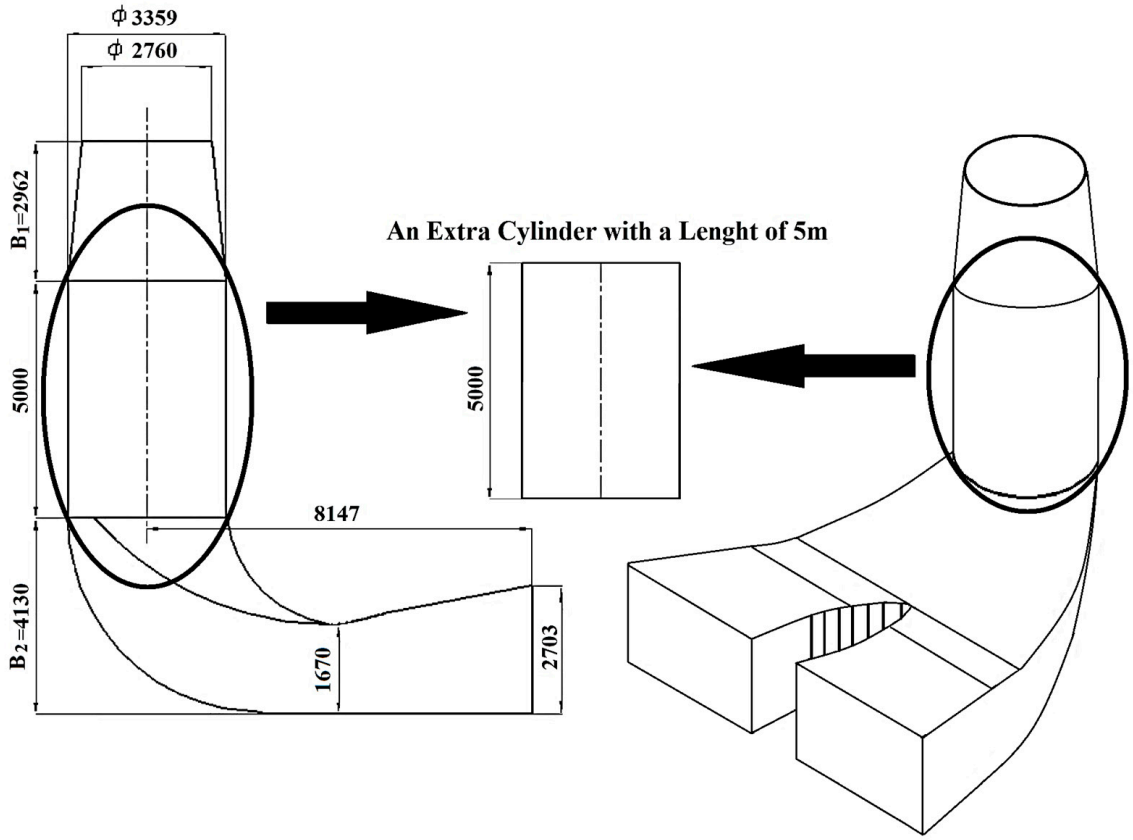

Figure 6. Maroon draft tube as-built dimensions (in millimeters).

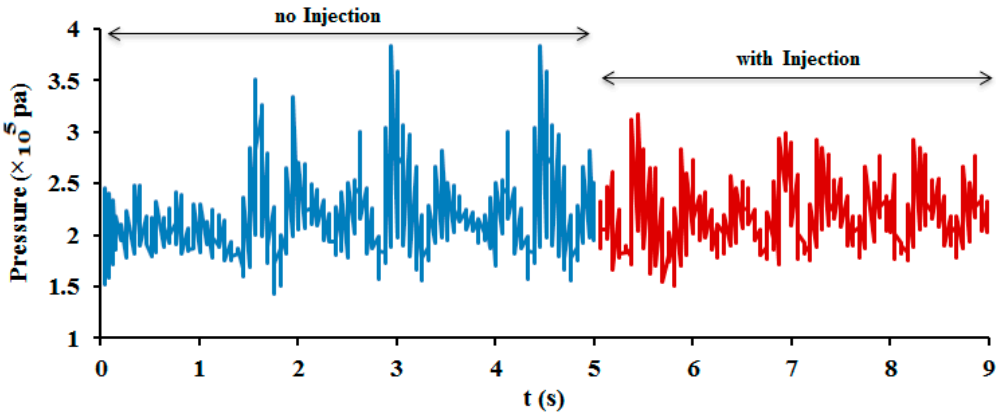

Figure 7. Pressure Fluctuations on the draft tube wall at 2.3 m below the draft tube inlet, at 86.2% operating point, by removing an extra 5 m.

Comparing Figures 4b and 7, it is evident that the injection technique is only influential in initially designed geometry, not as-built geometry. To further investigate this finding, simulations from a design perspective have compared as-built and initially approved design [36,37] sizes with dimensions obtained from Francis turbine empirical equations [5,38].

Therefore, using Equations (14)–(16), runner diameter and draft tube height (B1 in Figure 6) are calculated as follows [5,38]:

$$D_3 = 84.5 k_u \frac{\sqrt{H_n}}{n} \tag{14}$$

$$k_u = 0.31 + 2.5 \times 10^{-3} n_s \tag{15}$$

$$B_1 = \left(0.71 + \frac{62.8}{n_s}\right) \times D_3 \quad (16)$$

H_n, n, D_3, and n_s are the design head, runner speed in revolutions per minute, runner diameter, and specific speed, respectively.

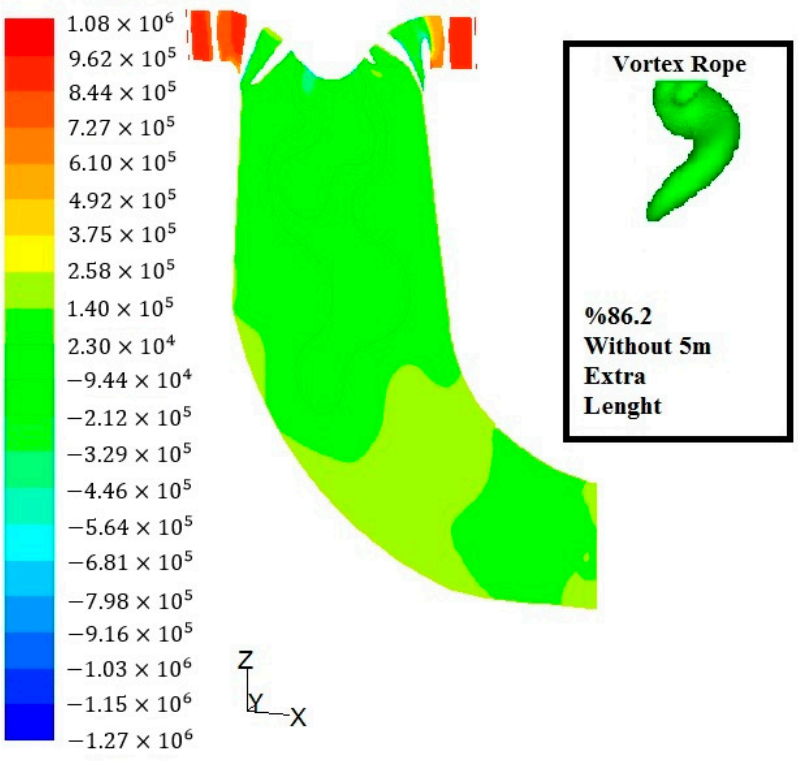

Figure 8. Axial static pressure contour and vortex rope at 86.2% operating point by removing an extra 5 m.

Calculated values from Equations (14) and (16) have been compared with as-built and initially designed dimensions in Table 6. Based on the mentioned equations, runner diameter, and draft tube height have a direct relationship. However, Table 6 shows that the draft tube height and runner diameter in the calculated and initially approved design dimensions have the same order. But in the as-built geometry, despite the increased draft tube height, the runner diameter has been kept constant, and the value of the draft tube dimension is approximately three times the runner diameter dimension. Therefore, based on CFD simulation and investigation of pressure fluctuations on the wall without and with injection in two geometries: as-built design and by removing extra parts in the draft tube, changes in turbine dimension can cause significant problems and endanger safety.

Table 6. As-built design, initially approved design, and calculated turbine dimensions based on Equations (14) and (16).

Dimensions	Calculated (mm)	Initially Approved Design (mm)	As-Built Design (mm)
Runner Diameter	2751	2393	2760
Draft tube height (B_1 in Figure 6)	2958	2415	7962 (2962 + 5000)

In addition to the above argument, the optimum proportions of Francis turbine draft tubes can be calculated based on the USBR standard. Accordingly, the optimum height of the draft tube, from the inlet draft tube to the elbow (h in Figure 9), is 2.5 times the runner

diameter [39]. Table 7 shows the calculated parameter "h" in Figure 9. As can be seen, the Maroon draft tube height is approximately 2.0 times higher than the standard height, which has caused unsafety and an unusual increase in pressure fluctuation after injection in this hydropower plant.

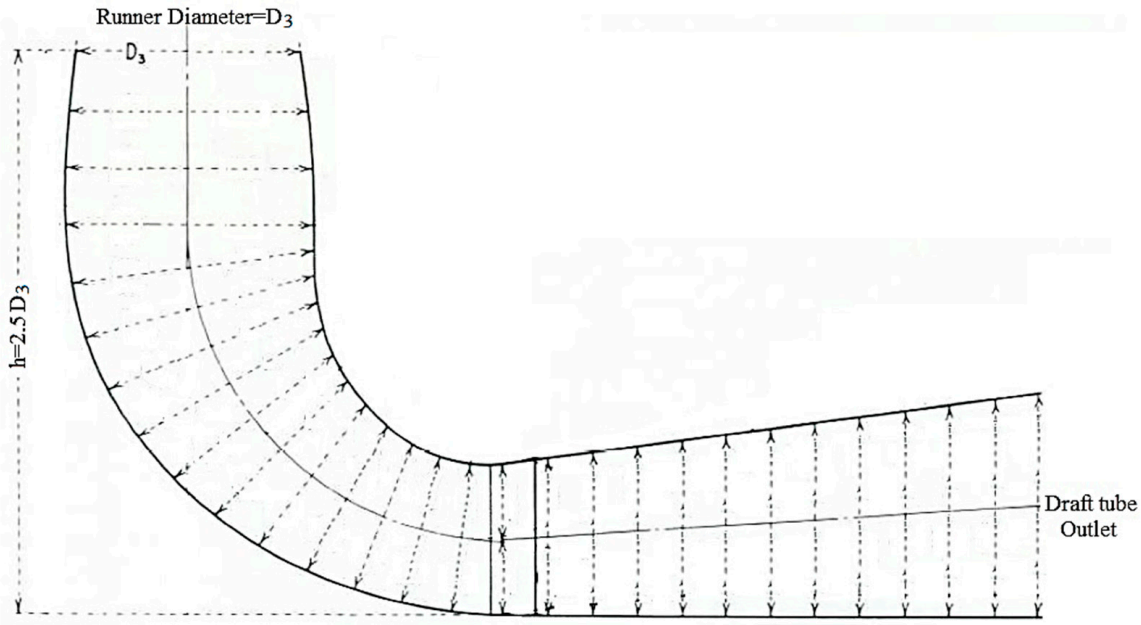

Figure 9. Draft tube height based on the USBR standard.

Table 7. As-built design and calculated draft tube height dimensions (based on the USBR standard).

Dimensions	Calculated (mm)	As-Built Design (mm)
Runner Diameter (D_3 in Figure 9)	2760	2760
Draft tube height (h in Figure 9)	6900	12,092 (2962 + 5000 + 4130)

4. Conclusions

This research examined the potential operational consequences of a slight change in the draft tube design parameters in the construction phase. Accordingly, the flow was simulated in a prototype turbine from the stay vanes to the draft tube outlet based on the SST k–ω turbulence model and a power-law discretization scheme in an unsteady state at three operating points: 66.6%, 86.2%, and 100%. Moreover, the effect of injection on pressure fluctuations was studied using air injection at two operating points: 86.2% and 100% from 72 nozzles on the perimeter of the draft tube from the discharge ring, and combined air and water injection at the 66.6% operating point. At the 66.6% operating point, air is injected, similar to the 86.2% and 100% operating points, and water is injected from the center of the runner cone.

The results show that, although injection is the commonly used method for reducing pressure fluctuations and vortex area, in the as-built geometry, the injection made pressure fluctuations worse, and this parameter was increased from 1.2 to 2.8 times at different operating points compared with one second after injection. Additionally, changing the air injection location from the draft tube's perimeter in the discharge ring to the center of the runner cone does not affect the decrease in pressure fluctuations. It increases the turbulence in the fluid, which shows the unexpected increase in pressure fluctuations is independent of the injection location. Nevertheless, the pressure fluctuations significantly decreased when the flow field was simulated in the initially approved design without and

with air injection. Consequently, the difference between the two geometries causes different responses to the injection.

Interestingly, the difference between the two geometries was slight in draft tube height. Accordingly, due to the topography difference between the draft tube outlets in the two hydropower units, 5 m was added to the draft tube height in the construction phase. Consequently, the slight change in the draft tube's height has dramatically affected its response to the injection technique. This finding agrees with the empirical Francis turbine dimension equations [38], where the runner diameter and draft tube height have a direct relationship. Consequently, when the draft tube height is changed in the construction phase, other corresponding parameters, including the runner diameter, must be adjusted; otherwise, serious operational problems can be expected, which can cause increasing operating and maintenance costs, decreasing hydropower efficiency, and significant challenges in using standard troubleshooting techniques.

Author Contributions: Conceptualization, M.M. (Moona Mohammadi); methodology, M.M. (Moona Mohammadi), M.M. (Mohammadreza Mohammadi); software, M.M. (Moona Mohammadi); validation, M.M. (Moona Mohammadi); formal analysis, M.M. (Moona Mohammadi); investigation, M.M. (Moona Mohammadi) and M.M. (Mohammadreza Mohammadi); resources, S.A. and A.M.; data curation, M.M. (Moona Mohammadi); writing—original draft preparation, M.M. (Moona Mohammadi); writing—review and editing, M.M. (Moona Mohammadi) and M.M. (Mohammadreza Mohammadi); visualization, M.M. (Moona Mohammadi); supervision, E.H. and M.B.-N.; project administration, E.H. and M.B.-N., M.M. (Moona Mohammadi). All authors have read and agreed to the published version of the manuscript.

Funding: This research received no external funding.

Data Availability Statement: Not applicable.

Acknowledgments: We appreciate the Shahid Chamran University of Ahvaz's support throughout the research and the Khuzestan Water & Power Authority (KWPA) research office's financial aid in publishing this work.

Conflicts of Interest: The authors declare no conflict of interest.

References

1. Yang, C.; Wu, J.; Xu, D.; Zheng, Y.; Hu, X.; Long, Z. Analysis of Flow characteristics and Pressure Pulsation in Horizontal Axis Double-Runner Francis Turbine. *Water* **2021**, *13*, 2671. [CrossRef]
2. Mohammadi, M.; Mohammadi, A.; Mohammadi, M. Optimizing Hydro Power Turbines in Order to Secure the Passage of Fishes in Khuzestan Province. *J. Appl. Comput. Mech. (JACM)* **2015**, *1*, 95–102. [CrossRef]
3. Junior, G.J.A.; Lima, A.K.F.; Vaz, J.R.P.; Lins, E.F. Computational Analysis of Vortex Rope in a Hydro Turbine of Tucurul Dam. *J. Braz. Soc. Mech. Sci. Eng.* **2020**, *42*, 313. [CrossRef]
4. Mosonyi, E. *Water Power Development High Head Power Plant*; Akademiai Kiado: Budapest, Hungary, 1991.
5. de Siervo, F.; de Leva, F. Modern Trends in Selecting and Designing Francis Turbines. *Water Power Dam Constr.* **1976**, *28*, 28–35.
6. Ruprecht, A.; Helmrich, T.; Aschenbrenner, T.; Scherer, T. Simulation of Vortex Rope in a Turbine Draft Tube. In Proceeding of the Hydraulic Machinery and Systems 21st IAHR Symposium, Lausanne, Switzerland, 9–12 September 2002.
7. Shetrok, S.; Suslov, D.; Skripkin, S.; Litvinov, I.; Gorelikov, E. An Overview of Active Control Techniques for Vortex Rope Mitigation in Hydraulic Turbines. *Energies* **2023**, *16*, 5131. [CrossRef]
8. Bosioc, A.L.; Szakal, R.A.; Stuparu, A.; Susan-Resiga, R. Numerical Analysis of the Flow by Using a Free Runner Downstream the Francis Turbine. *Int. J. Turbomach. Propuls.* **2023**, *8*, 14. [CrossRef]
9. Tucker, P.G.; Hewit, J.R. CFD Technique and their Relevant to Mechatronic. *Mechatronics* **1996**, *6*, 193–207. [CrossRef]
10. Saffarian, M.; Mohammadi, M.; Mohammadi, M. Non- Newtonian Shear- Thinning Fluid Passing Through a Duct with an Obstacle Using Power Law Model. *Stroj. Vestn.-J. Mech. Eng.* **2015**, *61*, 594–600. [CrossRef]
11. Foroutan, H.; Yavuzkurt, S. Flow in the Simplified Draft Tube of a Francis Turbine Operating at Partial Load-Part I: Simulation of the Vortex Rope. *J. Appl. Mech. Trans. ASME* **2014**, *81*, 061010. [CrossRef]
12. Foroutan, H. Simulation, Analysis, and Mitigation of Vortex Rope Formation in the Draft Tube of Hydraulic Turbines. Ph.D. Thesis, The Pennsylvania State University, State College, PA, USA, 2015.
13. Susan-Resiga, R.; Muntean, S.; Hasmatuchi, V.; Anton, I.; Avellan, F. Analysis and Prevention of Vortex Breakdown in the Simplified Discharge Cone of a Francis Turbine. *J. Fluid Eng. Trans. ASME* **2010**, *132*, 051102. [CrossRef]

14. Soni, V.; Roghelia, A.; Desai, J.; Chauhan, V. Design Development of Optimum Draft Tube for High Head Francis Turbine Using CFD In Proceeding of 37th International & 4th National Conference on Fluid Mechanics and Fluid Power, Madras/Chennai, India, 16–18 December 2010.
15. Maiwald, M.; Jester-Zürker, R.; Agostini Neto, A.D. Numerical Investigation of Francis Turbine Draft Tubes with Respect to Geometry Modification and Turbulence Treatment. In Proceeding of 25th IAHR Symposium on Hydraulic Machinery and Systems, Timisoara, Romania, 20–24 September 2010. [CrossRef]
16. Prasad, V.; Khari, R.; Chincholikar, A. Hydraulic Performance of Below Draft Tube for Different Geometric Configurations Using CFD. In Proceeding of the 8th International Conference on Hydraulic Efficiency Measurement (IGHEM), Roorkee, India, 21–23 October 2010.
17. Stefan, D.; Rudolf, P.; Skotak, A.; Motycak, L. Energy Transformation and Flow Topology in an Elbow Draft Tube. *Appl. Comput. Mech.* **2012**, *6*, 93–106.
18. Khare, R.; Prasad, V.; Verma, M. Design Optimisation of Conical Draft Tube of Hydraulic Turbine. *Int. J. Adv. Eng. Sci. Technol. (IJAEST)* **2012**, *2*, 21–26.
19. Jeon, J.H.; Byeon, S.S.; Kim, Y.J. Effects of Draft Tube on the Hydraulic Performance of a Francis turbine. In Proceeding of 6th International Conference on Pumps and Fans with Compressors and Wind Turbines, Beijing, China, 19–22 September 2013. [CrossRef]
20. Bajaj, R.; Khare, R.; Prasad, V. Effect of Diffuser Length on Performance Characteristics of Elbow Draft Tube with Dividing Pier. *Int. J. Mech. Eng. Technol. (IJMET)* **2014**, *5*, 1–12.
21. Khare, R.; Prasad, V.; Sharma, M. Numerical Simulation for Effect of Splitters On Performance of Elbow Draft tube. In Proceeding of International Conference on Hydropower for Sustainable Development, Dehradun, India, 5–7 February 2015.
22. Chakrabarty, S.; Sarkar, B.K.; Maity, S. CFD Analysis of the Hydraulic Turbine Draft Tube to Improve System Efficiency. *MATECH Web Conf.* **2016**, *40*, 02003. [CrossRef]
23. Agarwal, T.; Chaudhary, S.; Verma, S. Numerical and Experimental Analysis of Draft Tubes for Francis Turbine. *Indian J. Sci. Technol.* **2017**, *10*, 23. [CrossRef]
24. Nam, M.C.; Dechun, B.; Xiangji, Y.; Mingri, J. Design Optimization of Hydraulic Turbine Draft Tube Based on CFD and DOE Method. *IOP Conf. Ser. Earth Environ. Sci.* **2018**, *136*, 012019. [CrossRef]
25. Arispe, T.M.; de Oliveira, W.; Ramirez, R.G. Francis Turbine Draft Tube Parameterization and Analysis of Performance Characteristics using CFD Techniques. *Renew. Energy* **2018**, *127*, 114–124. [CrossRef]
26. White, F. *Viscose Fluid Flow*, 3rd ed.; McGraw-Hill: Singapore, 2006.
27. Chen, C.; Jaw, S. *Fundamentals of Turbulence Modeling*; Taylor & Francis Inc.: New York, NY, USA, 1997.
28. Subramanaya, S. *Hydraulic Mechanics*; Tata McGraw Hill Education Private Limited: New Delhi, India, 2013.
29. Mohammadi, M.; Hajidavalloo, E.; Behbahani-Nejad, M. Investigation on Combined Air and Water Injection in Francis Turbine Draft Tube to Reduce Vortex Rope Effects. *ASME J. Fluids Eng.* **2019**, *141*, 051301. [CrossRef]
30. Mohammadi, M. Simulation of Francis Turbine Draft Tube with Considering Air and Water Injection. Ph.D. Thesis, Shahid Chamran University of Ahvaz, Ahvaz, Iran, 2019.
31. *ASME V V 20, 2009*; The American Society of Mechanical Engineering, an American National Standard, Standard for Verification and Validation in Computational Fluid Dynamics and Heat Transfer. ASME PTC Committee: New York, NY, USA, 2009.
32. Melhavi, R.; MokariBehbahani, A.; Akhtarian, A.R. *Calibration of Maroon Hydro Power Plant Winter-Kennedy System*; Khuzestan Water & Power Authority: Behbahan, Iran, 2012.
33. Wu, Y.; Li, S.; Liu, S.; Dou, H.S.; Qian, Z. *Vibration of Hydraulic Machinery*; Springer Dordrecht Heidelberg: London, UK, 2013.
34. Dörfler, P.; Sick, M. *Flow-Induced Pulsation and Vibration in Hydroelectric Machinery*; Springer: London, UK, 2013.
35. Fraser, R.; Desy, N.; Demers, E.; Deschenes, C.; Fau, J.P.; Hamel, S. Improvements to Self-Venting Francis Turbines. In *Proceeding of Waterpower XIV*; HCI Publications: Kansas City, MI, USA, 2005.
36. GE Energy (UK) Limited. *Maroon Drawing Documents*; Khuzestan Water & Power Authority: Ahvaz, Iran, 2004.
37. GE Energy (UK) Limited. *Maroon Turbines Model Test Report*; Khuzestan Water & Power Authority: Ahvaz, Iran, 2000.
38. Mohammadi, M.; Mohammadi, M.; Mohammadi, A.; Farahat, S. Analyzing Mathematical and Software Methods for Selecting and Designing Fancies Turbine in Hydropower Plants. *J. Clean Energy Technol. (JOCET)* **2016**, *4*, 276–283. [CrossRef]
39. United State Department of the Interior BUREAU of Reclamation. A Water Resource Technical Publication Engineering Monograph No.20. In *Selecting Hydraulic Reaction Turbines*; Office of Design and Construction, Engineering and Research Center: Golden, CO, USA, 1976.